Future Foods 12 (2025) 100795

Contents lists available at ScienceDirect

Future Foods

journal homepage: www.elsevier.com/locate/fufo

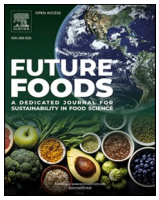

Plant-based alginate-guar gum-konjac glucomannan scaffold with enhanced thermal stability and biocompatibility for cultured meat production

Kuo-Hui Chiu [a,*], Szehon Anson Li [a], Stefan Schillberg [a,b], Che Julius Ngwa [a,*]

[a] Fraunhofer Institute for Molecular Biology and Applied Ecology IME, 52074 Aachen, Germany
[b] Institute for Molecular Biotechnology, RWTH Aachen University, 52074 Aachen, Germany

ARTICLE INFO

Keywords:
Biological compatibility
Edible scaffold
Hydrogel
Mechanical and structural integrity

ABSTRACT

Conventional livestock farming places a heavy burden on natural resources and contributes significantly to greenhouse gas emissions. As a sustainable alternative, cultured meat has gained significant attention; however, developing an effective scaffold for cultured meat production with both structural integrity and thermal stability remains a major challenge. This study presents a novel plant-based scaffold composed of alginate, guar gum, and konjac glucomannan, specifically engineered to improve the thermal stability required for cultured meat applications. The scaffold was fabricated using hydrogel formation, lyophilization, and autoclave sterilization to ensure its suitability for cell cultivation. Mechanical testing revealed an optimized scaffold with a young's modulus of approximately 93.45 kPa, closely resembling the stiffness of conventional meat. The scaffold demonstrated excellent water retention capacity and significantly enhanced thermal stability, retaining 86.8 % of its weight after cooking, overcoming a key limitation of traditional hydrogel-based scaffolds. Biocompatibility assessments confirmed that the scaffold is not cytotoxic to C2C12 myoblast cells, a mouse model cell line for cultured meat production, with CCK-8 assay results indicating strong cell viability. Additionally, live/dead staining of scaffolds with cultured C2C12 cells showed that over 80 % of cells remained viable, supporting its potential for long-term cell culture. These results highlight the scaffold's ability to maintain mechanical and structural integrity while providing a supportive environment for cell growth. In addition, myogenic marker MyoD1 was also accessed to confirm the great potential of cell differentiation within the scaffold. This study introduces an innovative scaffold formulation that enhances cultured meat processing by addressing thermal degradation challenges. By integrating plant-based biomaterials, this research paves the way for scalable, sustainable, and commercially viable cultured meat production, aligning with the future of food engineering and alternative protein development.

1. Introduction

Traditional livestock farming is a resource-intensive process, requiring vast acres of land, significant amounts of water, and substantial energy inputs. It is also a major contributor to greenhouse gas emissions particularly methane and carbon dioxide, which are critical drivers of global warming and environmental degradation (Steinfeld and Wassenaar, 2007). The search for alternative methods of meat production has become increasingly urgent to mitigate these environmental impacts and meet future food demands in a sustainable manner (Thavamani et al., 2020). Cultured meat is rapidly gaining attention as a sustainable and innovative alternative to traditional meat production, offering a potential solution to the environmental challenges posed by the conventional meat industry (Kirsch et al., 2023). It eliminates the need to raise and slaughter livestock, thereby significantly reducing land use and greenhouse gas emissions. Additionally, it also requires less water and eliminates the ethical concerns associated with factory farming (Jahir et al., 2023).

Despite its promise, a major challenge in cultured meat production is the development of effective scaffolds. These scaffolds provide the three-dimensional framework necessary for cells to attach, grow, differentiate, and form muscle tissue that closely mimics the texture and appearance of conventional meat (Levi et al., 2022). A critical factor in this process is the creation of an optimal scaffold that supports efficient cell cultivation. The scaffold serves as the structural foundation, providing a 3D microenvironment that is essential for cell growth and tissue formation,

* Corresponding authors.
E-mail addresses: kuo-hui.chiu@ime.fraunhofer.de (K.-H. Chiu), julius.ngwa.che@ime.fraunhofer.de (C.J. Ngwa).

https://doi.org/10.1016/j.fufo.2025.100795
Received 1 April 2025; Received in revised form 4 July 2025; Accepted 15 October 2025
Available online 17 October 2025

ultimately allowing the cells to develop into a meat-like structure (Seah et al., 2022). In addition to complying with FDA regulations, the scaffold must not only facilitate cell growth, but also be edible, ensuring both the safety and palatability of the final product (Post et al., 2020).

In this context, plant-derived biomaterials have emerged as an innovative and sustainable approach (Kim et al., 2024). Besides providing a biocompatible environment for cell growth, these materials help improve the overall efficiency of the cultivation process. Among these materials, alginate (Alg), a polysaccharide derived from marine brown algae, has shown immense potential as a scaffold for cultured meat (Savić Gajić et al., 2023). Its water solubility, excellent biocompatibility, and ability to form gels through simple ionic cross-linking make it particularly attractive for 3D cell culture applications (Seo et al., 2023; Chen et al., 2023). Alg has been extensively used in food and biomedical industries, showcasing its versatility as a biomaterial (Gheorghita Puscaselu et al., 2020; Ke et al., 2021). However, despite these advantages, Alg-based scaffolds face significant limitations, particularly with respect to thermal stability and cooking loss (Ko et al., 2021). During the cooking process, Alg scaffolds can lose their structural integrity, which is a critical drawback for their application in cultured meat. This phenomenon is attributed to the susceptibility of Alg to degradation under heat, resulting in compromised stability and an inability to maintain the intended texture of the cultured meat product. This limitation underscores the necessity for innovative scaffold designs that address the challenges of cooking loss while retaining the desirable properties of Alg.

Guar gum (GG) and konjac glucomannan (KGM) are two other promising plant-derived biomaterials. GG is a water-soluble food additive derived from the endosperm of *Cyamopsis tetragonolobus* and it offers excellent thickening, stabilizing, gelling, and emulsifying properties, and can preserve food quality and extend shelf life (Bhan et al., 2022; Mondal et al., 2024; Nabil et al., 2025; Madni et al., 2021). Similarly, KGM, extracted from the tubers of Amorphophallus konjac, has recently gained attention as an alternative biomaterial for cultured meat preparation, owing to its gelling and water retention capabilities (Ni et al., 2021; Redondo et al., 2023; Tang et al., 2024). The incorporation of GG and KGM alongside Alg may offer the potential to develop hybrid scaffolds with improved mechanical and thermal properties, addressing the limitations of Alg while leveraging its biocompatibility and ease of use. The plant-derived biomaterials hold particular appeal for the domain of cultured meat applications, given their FDA approval as food additives and their non-animal origin (Senturk Parreidt et al., 2018; A. Mortensen et al., 2017; A. Mortensen et al., 2017). Beyond regulatory compliance, their utilization aligns with the mounting demand for sustainable, ethical alternatives to animal-based materials. Moreover, their non-animal origin contributes to a substantial reduction in the environmental impact associated with conventional meat production, thereby mitigating ethical concerns surrounding animal exploitation.

This study proposes a novel strategy to address one of the challenges associated with cultured meat production through the development of plant-based scaffolds. A pivotal element of the research involves the incorporation of plant-derived biomaterials into the design of an advanced scaffold. This approach will promote efficient cell growth while simultaneously enhancing the thermal stability necessary for successful applications. The proposed scaffold is designed to address two critical challenges: biological compatibility and structural integrity during the cooking process. The objective is to ensure a final product that closely mimics conventional meat in texture, taste, and appearance through refining the properties of plant-based biomaterials and optimizing their application in scaffold design. By mitigating cooking loss and enhancing thermal stability, this research establishes the foundation for scalable and sustainable cultured meat production systems. The utilization of plant-derived biomaterials signifies a paradigm shift, offering a novel solution that aspires to create a more ethical, accessible, and environmentally sustainable food system. This approach signifies a substantial stride toward the development of a future where the production of cultured meat can meet global demand while concurrently minimizing environmental impact and ethical concerns.

2. Materials and methods

2.1. Scaffold preparation

Different combinations of plant-based materials including 1) 0.5 % w/v alginate (Alg); 2) 0.5 % w/v guar gum (GG); 3) 0.5 % w/v konjac glucomannan (KGM); 4) 0.5 % w/v alginate + 0.5 % w/v guar gum (AG); 5) 0.5 % w/v alginate + 0.5 % w/v konjac glucomannan (AK); 6) 0.5 % w/v guar gum + 0.5 % w/v konjac glucomannan (GK); 7) 0.5 % w/v alginate + 0.5 % w/v guar gum + 0.5 % w/v konjac glucomannan (AGK); 8) 0.5 % w/v alginate + 0.5 % w/v gelatin (AGel), were used to fabricate scaffolds. Briefly, alginate (Lianyungang Tiantian Seaweed Industrial Co., Ltd., China), guar gum (KoRo, Germany), konjac glucomannan (Vita2You, Germany) and gelatin (Fluka, Sigma-Aldrich, Germany) were dissolved in MiliQ water to get the desired concentration. One milliliter of each combination of solution (Alg, GG, KGM, AG, GK, AGK and AGel) was transferred into 48-well plates and 50 μL of 2 % w/v aqueous $CaCl_2$ (Sigma-Aldrich) was loaded directly to crosslink the hydrogel. After crosslinking for 24 h at room temperature, the hydrogel underwent gelation, forming a cylinder with a diameter and height of 10 mm. The hydrogels were frozen at −80 °C overnight and subsequently lyophilized by the freeze-dryer (VaCo5, ZIRBUS, Germany) for 72 h to fabricate the scaffolds. The lyophilized scaffolds were then stored in a vacuumed desiccator to keep them dry.

2.2. Characterizations of scaffolds

2.2.1. Scaffold water uptake

For scaffolds to be used for cell culture, they need to be able to absorb cell culture medium in order to supply the nutrients needed for the seeded cells to proliferate. For this reason, the ability of the scaffold to take up water was tested. This was done by analyzing the weight of the scaffold before and after incubation with PBS for 24 h. The water uptake ability was calculated from the mass fold-change by the following equation:

$$Water\ uptake = (W_w - W_D)/W_D \times 100\% \quad (1)$$

where W_D represented the dry sample and W_W represented the weight of the scaffolds after PBS incubation.

2.2.2. Scaffold degradation and thermal stability test

The stability of the scaffolds was measured by the wet-weight and dry-weight analysis after incubation in PBS. The samples were incubated in 1 mL PBS in a 24-well plate at room temperature, and weighted after one, three, and five days. The stability ratio was calculated from the following equation:

$$Swelling\ ratio = (W_t / W_1) \times 100\% \quad (2)$$

where W_t and W_1 represented the weight of samples treated at different time points and the samples pre-incubated in PBS for one hour, respectively. After the W_t was measured, the treated samples were frozen directly at −80 °C and lyophilized to get the dry weight of the sample matrix.

The thermal stability was also evaluated by cooking on a hot plate at 180 °C for 5 min on each side and determining the weight loss. The weight loss ratio was calculated from the following equation:

$$Weight\ loss\ ratio = (W_a - W_b)/W_a \times 100\% \quad (3)$$

where W_a is the weight before cooking, and W_b the weight after cooking.

2.2.3. Scaffold mechanical stability

Prior to testing, the scaffolds were rehydrated in 500 μL of PBS for a period of 24 h. The stress-relaxation test was initially conducted using a universal testing machine (Minizwick, ZwickRoell, Germany). All samples were first subjected to a tare load of 0.05 N to allow for equilibrium to be reached. Subsequently, the scaffolds were subjected to a 20 % strain at a strain rate of 4 mm/s, followed by a 300-second holding period to determine the stress relaxation behavior. The stress relaxation behavior of the hydrogels was analyzed by fitting the experimental data to an exponential decay model. The relaxation curve was described using the following equation:

$$\sigma(t) = \sigma_0 e^{-t/\tau} \tag{4}$$

where $\sigma(t)$ is the stress at the time t, σ_0 is the initial stress immediately after applying strain, and τ is the relaxation time constant, which characterizes the rate of stress decay (Chiu et al., 2023). The decay rate (λ) was calculated by the reciprocal of the relaxation time constant.

Afterwards, dynamic compressive loading was applied up to 40 % strain at a strain rate of 4 mm/s to determine the stiffness. Consequently, the Young's modulus (E) of the samples was calculated with the range between 0 % to 20 % strain using the formula:

$$E = \frac{\sigma}{\epsilon} = \frac{F/A}{\Delta l/l_0} \tag{5}$$

where σ is the compression stress, and ε is the compression strain. The stress was calculated using the standard force (F) applied to the samples, with the cross-sectional area (A) taken as the denominator. The strain of compression was calculated using the deformation (Δl) divided by the original length (l_0). The mean value of the Young's modulus for each scaffold was calculated based on the data obtained from three individual samples (Chiu et al., 2023).

2.2.4 Scanning electron microscopy analysis

2.3. Cell maintenance and cultivation in scaffold

Mouse myoblast cell line C2C12, was maintained in tissue culture flask with Dulbecco's modified Eagle's medium (DMEM, PAN-Biotech, Germany) containing 10 % v/v fetal bovine serum (FBS, PAN-Biotech, Germany) in an atmosphere of 5 % CO_2 at 37 °C. The cells were passaged when they reached 80 % confluency. Culture medium was changed twice a week to maintain the cell growth.

To cultivate the cells in scaffolds, C2C12 cells were trypsinized and seeded by directly injection into the scaffolds with a concentration of 1 × 10^6 cells/50 μL and incubated for 2 h to allow for cell attachment (Chen et al., 2015). After the initial incubation, scaffolds were then transferred into a new 48-well non-tissue culture plate with 500 μL fresh medium for continuously cultivation. The culture medium was changed twice a week to maintain the cell growth.

2.4. Scaffold biocompatibility

The scaffold biocompatibility was determined by indirectly assessing the cytotoxicity of the medium in which the scaffolds have been incubated on C2C12 cells using the CCK-8 assay (Cell Counting Kit-8, Sigma-Aldrich) as described by the manufacturer. To this end, the scaffolds were incubated in fresh culture medium for 24 h, and the supernatants were collected as condition medium. Meanwhile, 1.5 × 10^5 cells/mL were seeded in 48-well tissue culture plates and also incubated in fresh culture medium for 24 h. Afterward, the medium was discarded and replaced by the condition medium to evaluate the cytotoxicity. After 24 h cultivation, the cells cultivated with condition medium were washed with PBS and the CCK-8 assay was performed. The CCK-8 assay working solution was prepared by first diluting the stock solution in the cell medium (1:10) and subsequently incubating the samples for 4 h at 37 °C. Subsequent to the incubation period, the collected supernatant was subjected to spectrophotometric analysis at a wavelength of 450 nm using a microplate reader (Epoch, BioTek, Germany).

The cell viability following incubation of C2C12 cells directly on the scaffolds was also determined. To do this, the scaffolds were incubated with C2C12 cells and after one day and seven days of cultivation, the scaffolds were staining with 4 μM calcein-AM, which labels live cells, and 4 μM propidium iodide (PI) (BioLegend, USA), which labels dead cells, to evaluate the cell viability. After 1 h of staining, the cells cultured within the scaffolds were visualized and digital images were taken using a fluorescence microscope. Live cells exhibited green fluorescence due to calcein-AM (excitation/emission: 495 nm/515 nm), while dead cells displayed red fluorescence as stained by the Aqua-fluorescent reactive dye PI (excitation/emission: 540 nm/615 nm). Images were analyzed from three random positions in at least three individual samples using the ImageJ software by measuring the fluorescence signal of live cells (green) and dead cells (red). For analysis, all images were converted to 8-bit grayscale and the threshold was automatedly adjusted to the segment fluorescence signals. The live cell ratio was calculated using the formular:

$$\textit{Live Cell ratio}\ (\%) = \left(\frac{\textit{Live cells}}{\textit{Live cells} + \textit{Dead cells}}\right) \times 100\% \tag{6}$$

Where live cells represent the number of spots detected in the green channel stained with calcein-AM fluorescence dye and dead cells represent the number of spots detected by the red PI fluorescence dye. Data from individual samples were pooled to calculate mean values and standard deviations.

2.5. Cell differentiation and analysis

To evaluate the cell differentiation, 5 × 10^6 C2C12 cells were seeded per scaffold and cultivated for three days for adaptation. Afterward, control medium (DMEM + 10 % FBS) and differentiation medium (DMEM + 2 % Horse serum) was used to promote the cell differentiation for four days. The samples were then collected and immunofluorescence staining was performed to visualize the myogenesis early marker MyoD1.

For immunostaining, the samples were fixed with 4 % formaldehyde overnight at 4 °C, and then washed three times with PBS and the cell in the samples were permeabilized using 0.2 % v/v Triton X-100 (Fluka, Germany) for one hour, and non-specific binding sites were then blocked by incubation in 3 % w/v bovine serum albumin solution (BSA; Sigma-Aldrich) for 2 h at RT with shaking. Samples were incubated overnight at 4 °C with MyoD1 primary antibody (rabbit, 1:400, A0671, ABclonal, Germany) in 2 % w/v BSA/PBS solution to label the corresponding protein. After washing three time with PBS, the samples were incubated at RT for 3 h in the dark with a mix of the secondary antibody Alexa Fluor 594 (goat-anti rabbit, 1:1000, Abcam, UK) and phalloidin (1:400, Alexa Fluor 488 Phalloidin, Thermo Fisher Scientific) in 2 % w/v BSA/PBS solution and then washed three times with PBS. The protein expression and signal localization were investigated using Keyence fluorescence microscope (BZ-X800, Keyence, Germany).

2.6. Statistical analysis

All experiments were conducted in triplicate, with three biological replicates ($n = 3$) per experiment. The data were expressed as the mean ± standard deviation. The statistical analysis was conducted using one-way (swelling ratio, degradation, stiffness, and cell viability) or two-way ANOVA (CCK-8), with the software Graphpad Prism 10 (GraphPad Software LLC, USA). A p-value of less than 0.05 was considered to indicate a statistically significant result; otherwise, the result wasn't labelled specifically). Significant levels were indicated by the symbols $p < 0.05$ (*), $p < 0.01$ (**), $p < 0.005$ (***), and $p < 0.001$ (****), or the compact letter display, in which different letters indicate significant

differences between groups ($p < 0.05$). Groups sharing the same letter are not significantly different from each other.

3. Results

3.1. Scaffold material characteristic

The scaffold composition is a critical factor which affect its characteristic. A concentration of 0.5 % w/v of each component was chosen based on a preliminary testing where different concentrations of the components (0.5 % w/v, 1 % w/v, 2 % w/v) were tested. Higher concentrations posed significant challenges in mixing due to the high viscosity of the mixture. The two essential mechanical properties of cell scaffolding are hydrophilicity and material stability. Scaffolds of varying compositions were fabricated and then immersed in PBS for 24 h to assess their ability to absorb water and degree of stability. The morphology of the scaffolds was first determined by visual inspection prior to and following immersion in PBS (Fig. 1A-C) The scaffolds GG and GK were completely soluble in PBS thereby indicating an unsuccessful cross-linking (Fig. 1B, C). The remaining scaffolds exhibited re-swelling capacity (Fig. 1C). However, the scaffold KGM displayed a minimal degree of cross-linking, resulting in a malleable consistency akin to a slime (Fig. 1C).

The quantified water uptake capacity of the scaffolds was depicted in Fig. 2. GG and GK scaffolds were excluded as they completed dissolved in PBS therefore, they did not meet the criteria for a scaffold. The water uptake ability of the other scaffolds was evaluated by comparing their dry weight and wet weight after 24 h PBS incubation (Fig. 2A). The scaffolds were able to absorb with approximately 24.9-fold (Alg), 28.1-fold (KGM), 24.02-fold (AG), 24.58-fold (AK), 28.1-fold (AGK), 21.17-fold (AGel) water relative to their dry weight (Fig. 2B). All groups of scaffolds revealed great capacity of water holding ability, proofing the property as a scaffold for cell cultivation.

3.2. Stability and swelling property

As a scaffold for cell cultivation, stability is one of the critical factors to offer a stable microenvironment for 3D cultivation. Scaffold stability was assessed by two key aspects: swelling ability and matrix degradation. The swelling ratio results demonstrate the ability of the scaffolds to absorb and retain water within 5 days of incubation (Fig. 3A). Among the samples, AGK showed the highest swelling ratio of 333 %, highlighting its superior water absorption capacity. Although a slight decrease in swelling ratio was observed after 3 and 5 days of incubation, the changes were not statistically significant and AGK retained its position as the best performing scaffold in terms of swelling capacity. All the other scaffolds including Alg, KGM, AG, AK and AGel revealed moderate swelling capacity without significantly different (compare to the wet weight of the scaffolds). These results highlight the critical role of material composition in influencing the swelling behavior of the scaffolds, with AGK being particularly effective in water retention.

To evaluate matrix degradation, the scaffolds were lyophilized and the dry weight was analyzed after swelling ratio measurement (Fig. 3B). Most of the scaffolds show no significant mass loss after five days of incubation, confirming that their stability is not affected by degradation of the matrix itself. This trend indicates that while swelling ability varies between materials, the majority of scaffolds remain stable in terms of matrix integrity. konjac glucomannan; AG: alginate-guar gum; AK: alginate-konjac glucomannan; AGK: alginate-guar gum-konjac glucomannan; AGel: alginate-gelatin. The experiment was conducted on three individual replications and utilized the statistical analysis to access the data at varying time points for each group. The results without statistic labelled revealed no statistically significant difference.

Thermal stability is a crucial property for cultured meat scaffold. A good thermal stability is needed to offer a lower loss of the cultured meat during the cooking process. An analysis was conducted to evaluate the thermal stability of the scaffolds before and after the cooking process (Fig. 4). The initial weights of the scaffolds before cooking varied across different material compositions, as shown in the figure. After cooking, the Alg scaffold exhibited the greatest weight loss, with a reduction from 177 mg to 20 mg, corresponding to 88.7 % weight loss, demonstrating its significant degradation and poor thermal stability (Fig. 4). The AG scaffold demonstrated a substantial weight reduction of 71.4 %, with a decrease from 280 mg to 80 mg. In addition, the AGel scaffold also exhibit a 72.3 % of weight loss with the decrease from 253 mg to 70 mg after the cooking process. In comparison, the AK scaffold exhibited a

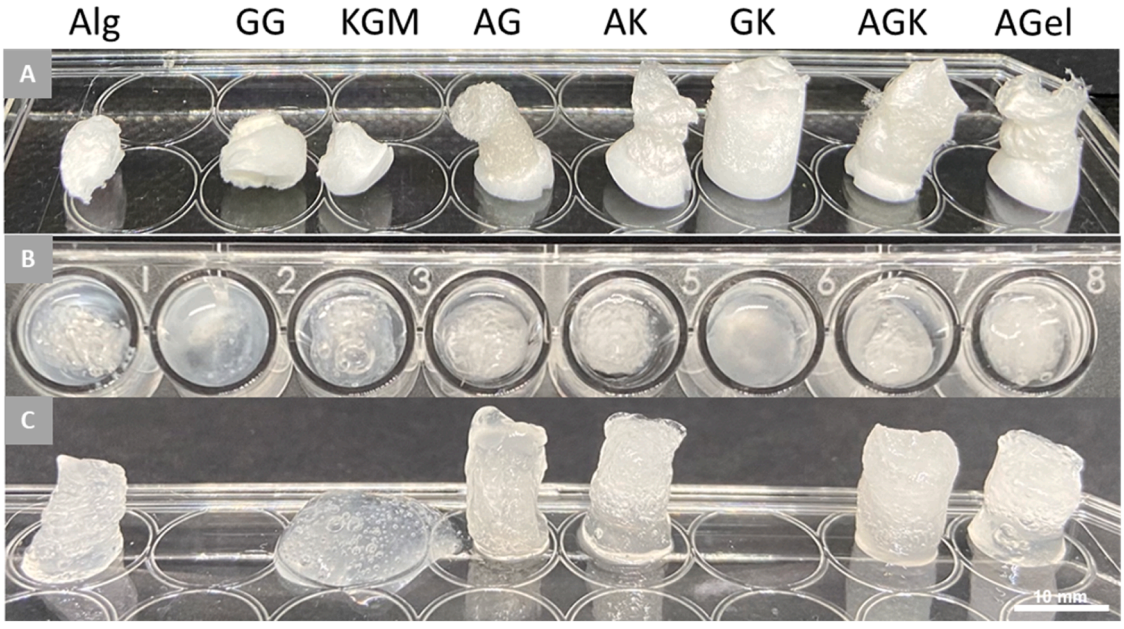

Fig. 1. Scaffolds morphology after lyophilization and re-swelling (A) Scaffolds morphology after 72 h lyophilization. (B and C) The scaffolds after immersion in PBS for 24 h, (B) top view and (C) front view, only scaffolds that remained intact are shown. Abbreviations: Alg: alginate; GG: guar gum; KGM: konjac glucomannan; AG: alginate-guar gum; AK: alginate-konjac glucomannan; GK: guar gum-konjac glucomannan; AGK: alginate-guar gum-konjac glucomannan; AGel: alginate-gelatin, Scale bar: 10 mm.

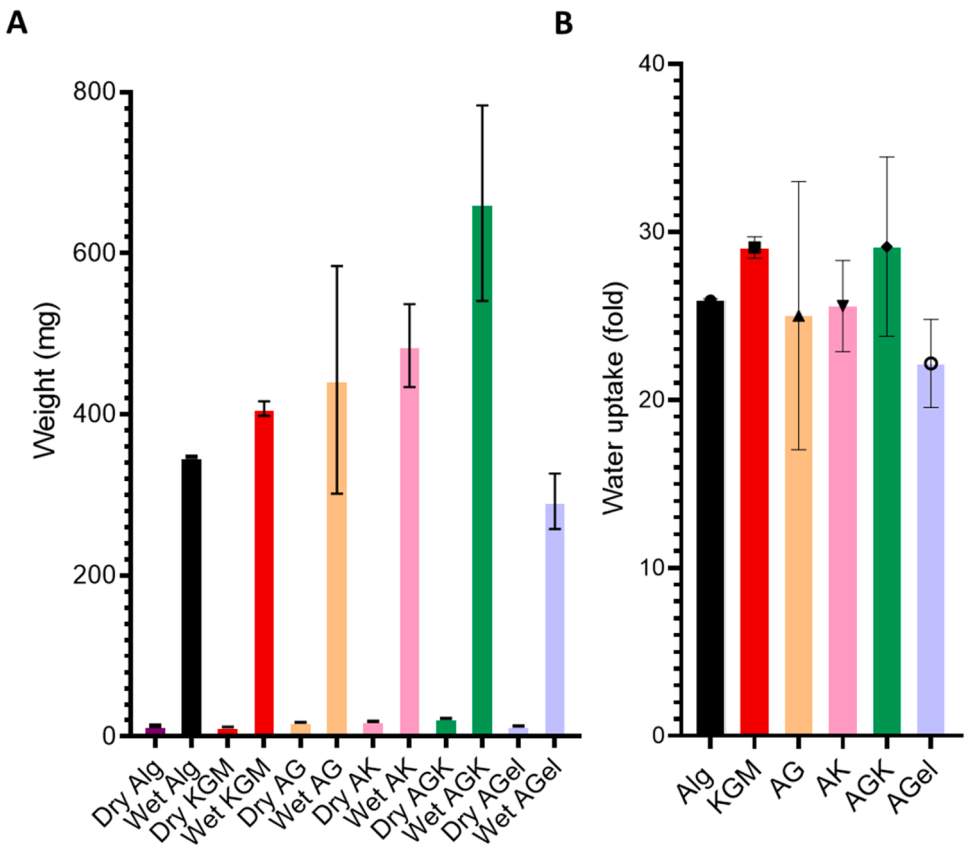

Fig. 2. Water uptake ability of scaffolds The water uptake ability of the scaffolds was determined by comparing the (A) dry weight (Dry) and wet weight (Wet) as well as (B) the fold changed of the scaffolds after 24 h incubation in PBS. Alg: alginate; KGM: konjac glucomannan; AG: alginate-guar gum; AK: alginate-konjac glucomannan; AGK: alginate-guar gum-konjac glucomannan; AGel: alginate-gelatin. Three independent experiments were performed in triplicate and subsequently normalized to its initial weight to calculate the changing ratio. The results without statistic labelled revealed no statistically significant difference.

slightly reduced weight loss of 55.6 %, decreasing from 293 mg to 130 mg. Interestingly, the AGK scaffold exhibited the least weight loss among the materials, with only 13.2 % of its mass lost, decreasing from 345 mg to 300 mg. This suggests that AGK has superior thermal stability and structural integrity compared to the other tested scaffolds. These findings emphasize the thermal resilience of the AGK scaffold, making it a promising candidate for applications requiring stability under heat exposure as cultured meat scaffold.

3.3. Scaffold stiffness and stress-relaxation property

The mechanical properties of the scaffolds, including stiffness and stress relaxation, are critical parameters that can influence cell adhesion and drive differentiation. The mechanical characteristics of the scaffolds were evaluated using a universal compression testing machine. The stiffness was measured by compressive stress-strain analysis, illustrating the stress-strain diagram (Fig. 5A). AGK exhibited the highest values of young's modulus (93.45 kPa) at the strain levels 0 % to 20 %, demonstrating superior stiffness compared to the other scaffold groups (Fig. 5B). Alg showed remarkable stiffness (79.38 kPa), ranking just below AGK, while AGel (23.91 kPa) and AG (25.31 kPa) showed moderate stiffness. AK had the lowest stress response (16.11 kPa), indicating the weakest mechanical performance. The result quantified the compressive modulus, confirming that AGK significantly outperformed the other scaffolds, followed by Alg, while AK had the lowest mechanical strength.

The stress relaxation property of the scaffolds was analyzed (Fig. 5C) and quantified the relaxation behavior by relaxation time constant (Fig. 5D) to evaluate the viscoelastic property over time. The higher decay rate indicated the faster stress relaxation. Alg exhibited the highest decay rate (0.147 %) followed by AGK (0.139 %), AG (0.131 %), AK (0.129 %), and AGel (0.117 %). These results suggested that all scaffolds revealed great viscoelastic property, while AGK and Alg indicated faster stress relaxation.

3.4. Scaffold biocompatibility

The cultivation of cells within a scaffold is contingent upon the material's biocompatibility. The assessment of the scaffold's cytotoxicity was conducted through indirect cultivation. The supernatant after scaffold pre-incubation was used for cell cultivation for 24 h, as described previously. The results show that all groups exhibited high levels of biocompatibility, with cell metabolic activity exceeding 80 % in all seven groups (Fig. 6A). The cell viability didn't show any significant different among all groups. To assess the direct effect of cell cultivation on the scaffolds, the AGK scaffold was selected, as it demonstrated the best performance in terms of stiffness, stability, and low cytotoxicity, making it optimal for cultured meat production. Alg was utilized as the negative control, while AGel served as the positive control due to its inherent gelatin content, which promotes cell attachment. The internal structure was also depicted via scanning electro microscope (SEM) and illustrated the scaffold architecture (Figure S1). The cells were then cultivated directly within the Alg, AGK, and AGel scaffolds, and cell viability was evaluated via live/dead staining analysis after one day and seven days of cultivation (Fig. 6B). The over view of cell viability after seven days cultivation was illustrated in lower magnification imaging (Figure S2). The results revealed predominantly green fluorescence for live cells across all scaffolds, with minimal red fluorescence indicating less dead cells. After one day and seven days of cultivation, the AGK scaffold supported high cell viability, with over 80 % live-cell ratios

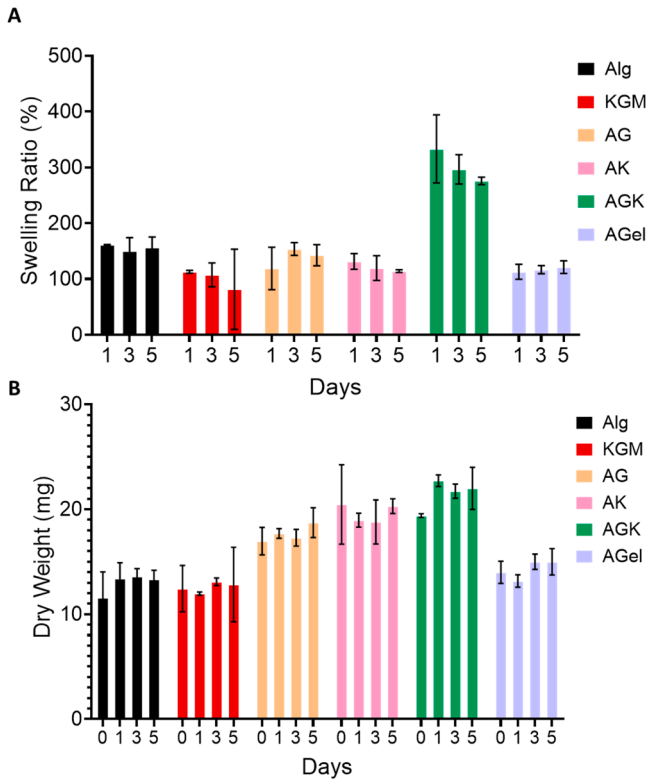

Fig. 3. Scaffolds stability in terms of swelling and degradation (A) The swelling ratio of the scaffolds on days 1, 3, 5 was measured by wet weight and normalized to the scaffold on day 0, which was incubated in PBS for one hour. After measuring the wet weight, the scaffolds were frozen at −80 °C and lyophilized to measure the dry weight. (B) The dry weight of the scaffolds was then analyzed to indicate the degradation of the scaffolds. Alg: alginate; KGM.

quantified using ImageJ signal intensity analysis. The results suggested that the AGK scaffold offered a biocompatible microenvironment for cell growth, with its performance matching or exceeding that of the gelatin-based positive control (AGel). Additionally, the stability and effectiveness of the plant-derived scaffolds make them promising candidates for cultured meat production.

3.5. *Cell differentiation potential on scaffolds*

In order to assess the differentiation potential of C2C12 cells on the scaffolds, the scaffold containing the cells were first cultured for three days in a growth medium to allow for adaptation. Thereafter, the scaffolds were transferred to differentiation medium and cultivated for an additional four days. As shown in Fig. 7, the expression of the myogenic early marker MyoD1 was significantly increased under differentiation conditions compared to the control. In the control group, cells exhibited low MyoD1 expression and appeared more randomly distributed. Conversely, cells exposed to the differentiation medium exhibited augmented MyoD1 levels and a more aligned morphology (Fig. 7A). Quantitative analysis confirmed significantly higher MyoD1 expression in the differentiation groups, thereby demonstrating the scaffold's ability to support myogenic differentiation (Fig. 7B). A notable finding was the substantially elevated level of MyoD1 expression observed in the AGK scaffold in comparison to the Alg scaffold under identical differentiation conditions. This observation indicated that the AGK scaffold may promote the development of a more favorable microenvironment for myogenesis.

4. Discussion

Cultured meat has recently emerged as an innovative and sustainable alternative to traditional meat production, offering significant environmental benefits and high potential for transforming the future food industry. A critical component in cultured meat production is the development of sustainable scaffolds to support cell growth and tissue formation. Plant-derived biomaterials present a promising solution, providing sustainable, ethical, and scalable alternatives to animal-based

	Alg	KGM	AG	AK	AGel	AGK
Before cooking			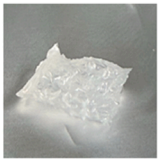		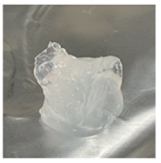	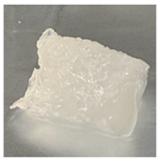
Weight	177 mg	183 mg	280 mg	293 mg	253 mg	345 mg
After cooking	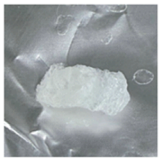	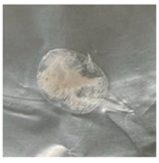	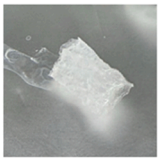	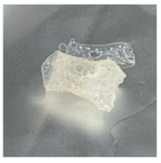	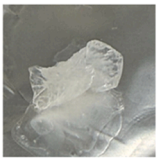	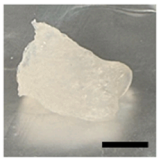
Weight	20 mg	-	80 mg	130 mg	70 mg	300 mg
Weight loss %	**88.7%**	**-**	**71.4%**	**55.6%**	**72.3%**	**13.2%**

Fig. 4. Thermal stability of different scaffolds before and after heat-treatment. The images showed the visual appearance of Alg, KGM, AG, AK, AGel, and AGK scaffolds before cooking (top row) and after cooking at 180 °C for 5 min each side (bottom row), with their respective weights recorded. The weight loss percentages were calculated to evaluate the stability of each scaffold after the cooking process. Alg: alginate; KGM: konjac glucomannan; AG: alginate-guar gum; AK: alginate-konjac glucomannan; AGK: alginate-guar gum-konjac glucomannan; AGel: alginate-gelatin. The thermal stability was tested three times and each time with three samples for each group. The experiment was conducted on three individual replications with three samples for each replication.

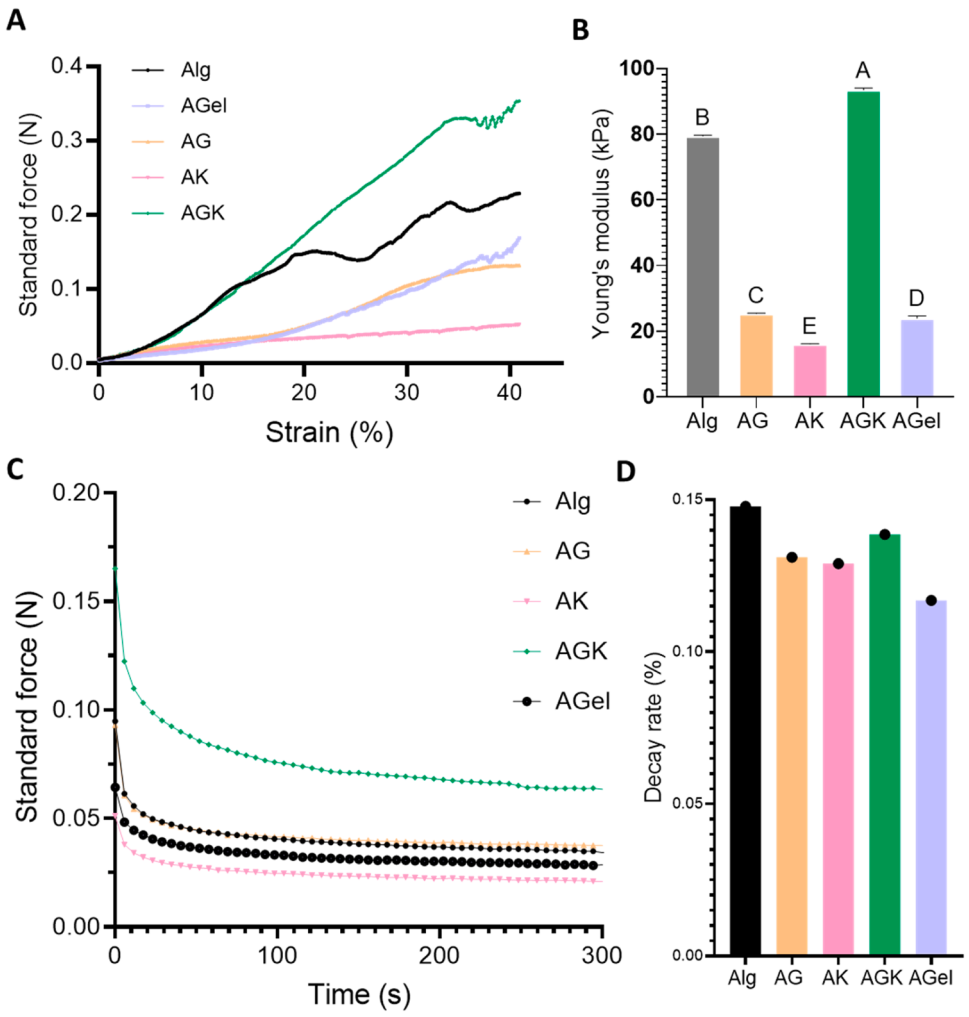

Fig. 5. Materials characteristics (A) Compression Stress-Strain curves of various scaffolds after one day swelling in PBS. (B) The stiffness of the scaffolds was calculated as Young's modulus. The presence of different letters above the bars signifies statistically differences between groups ($p < 0.05$), as determined by one-way ANOVA. Conversely, groups sharing the same letter are deemed to be non-significantly different from each other. (C) Scaffold relaxation property was analyzed by applying a standard 20 % strain and measure the force applied on the scaffold within 300 s. (D) The relaxation behavior was then quantified by relaxation time constant to indicate the decay rate of the scaffolds. Alg: alginate; KGM: konjac glucomannan; AG: alginate-guar gum; AK: alginate-konjac glucomannan; AGK: alginate-guar gum-konjac glucomannan; AGel: alginate-gelatin. The experiment was conducted on three individual replications.

scaffolds. In this study, we investigated various combinations of three widely used food-grade materials (alginate, guar gum, and konjac glucomannan) to identify an optimal formulation for cultured meat scaffolds. The results demonstrated that combining 0.5 % w/v alginate, 0.5 % w/v guar gum and 0.5 % w/v konjac glucomannan results in the production of scaffolds which support cell growth while delivering excellent mechanical properties, highlighting their suitability for use in cultured meat production.

To identify the optimal scaffold for cultured meat production, various combinations of biomaterial scaffolds were first prepared as hydrogels and then lyophilized to create porous structures. This lyophilization process improved both the permeability and mechanical properties of the scaffolds, which are essential for supporting cell growth and mimicking the structural integrity of natural tissues (Naahidi et al., 2017). The porous design not only facilitates nutrient and oxygen diffusion but also allows the scaffold to withstand mechanical force stimulation, addressing the inherent brittleness of traditional hydrogels. A critical attribute of an effective scaffold is its stability during the production process, which ensures the maintenance of its structural integrity and mechanical properties throughout the cell cultivation period. This stability prevents degradation that could potentially compromise cell adhesion and growth. The GG, GK, and to a lesser extent the KGM scaffolds exhibited high dissolution in PBS. However, when alginate was incorporated to produce the AG, AGK, and AK scaffolds, respectively, the resulting scaffolds were relatively stable. This suggests that GG, GK, and KGM interact poorly with Ca^{2+}, leading to weak crosslinking (Fu et al., 2018). In contrast, the addition of alginate, which has a strong affinity for Ca^{2+}, enhances crosslinking and significantly improves scaffold stability. The scaffold's water uptake ability is also crucial, as it facilitates the creation of an optimal microenvironment for cell proliferation and differentiation. A scaffold with high water uptake capacity can effectively mimic the extracellular matrix by providing cells with adequate hydration and creating favorable conditions for their growth and development. However, highly hydrated scaffolds, such as those based on alginate, often demonstrate inadequate stability when subjected to heat stimulation (Ko et al., 2021). For scaffolds intended for cultured meat applications, thermal stability is crucial due to the cooking process required to render the product edible. To address this, researchers commonly incorporate protein-based materials to enhance polymerization and stabilize the matrix structure under heat (Wannasin et al., 2024). Surprisingly, the AGK scaffold exhibited exceptional thermal stability, successfully overcoming the challenge of matrix degradation during the cooking process. This property renders AGK a promising candidate for use in cultured meat applications,

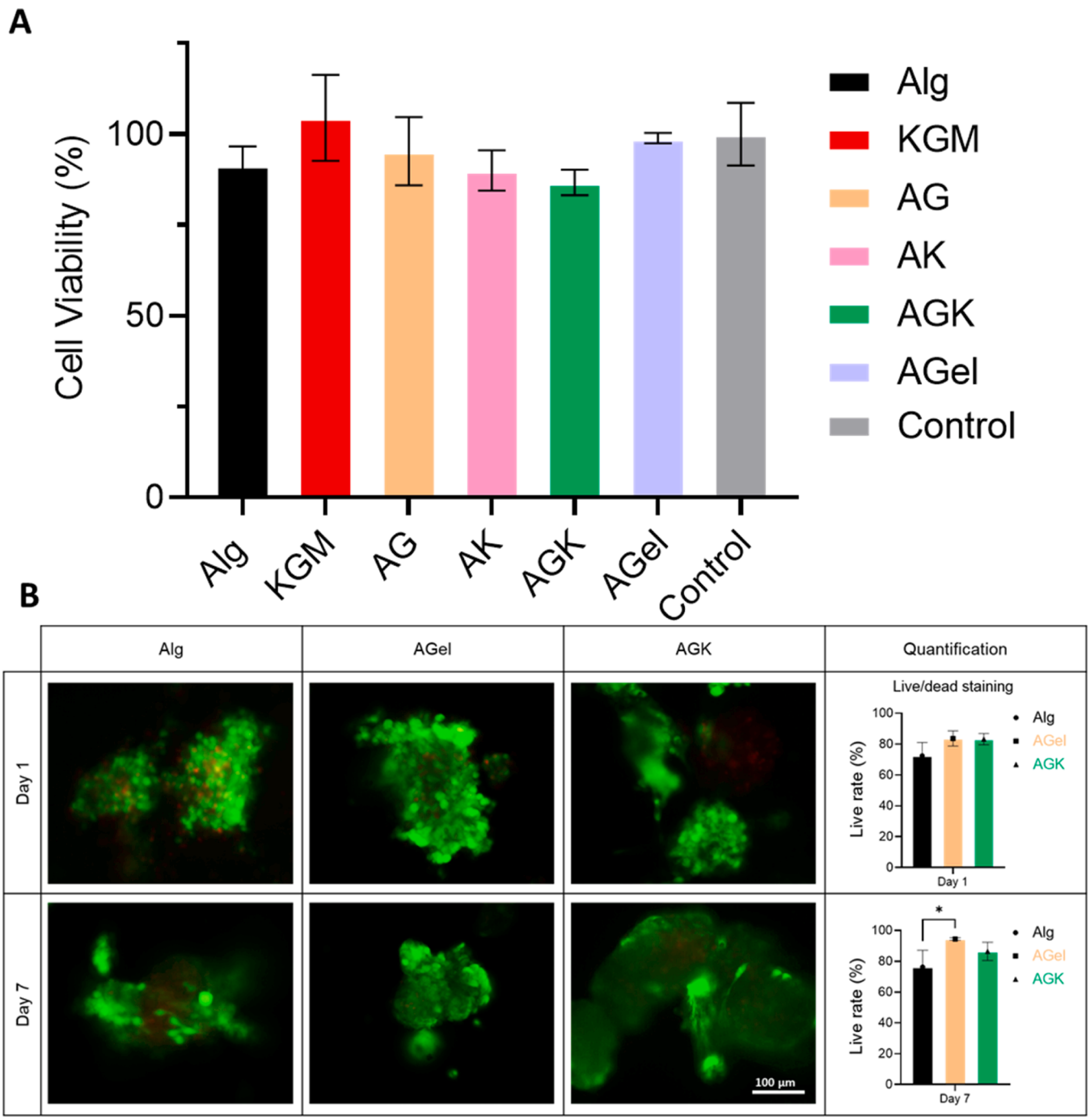

Fig. 6. Evaluation of biocompatibility and cell viability of plant derived scaffolds. (A) Cell cytotoxicity of scaffolds was analyzed by CCK-8 assay after 24 h indirect co-cultivation. All scaffolds showed high biocompatibility, with no significant differences in cell metabolic activity observed among the groups. (B) Representative live/dead staining images of cells cultured on scaffolds showing green fluorescence using calcein-AM for live cells and red fluorescence with propidium iodide for dead cells after 1 day and 7 days. Quantified live cell ratios from live/dead staining was performed by ImageJ. Scale bar: 100 μm, applied to all six fluorescence figures. The experiment was conducted on three individual replications. *: $p < 0.05$. No labelled between groups represented p value > 0.05.

ensuring both functionality and practicality in applications relevant to actual use.

A comprehensive analysis was conducted to evaluate the material properties and their impact on a mouse myoblast C2C12 cell line. The AGK scaffold demonstrated exceptional mechanical properties, exhibiting a Young's modulus of approximately 93.45 kPa, which closely approximates the mechanical characteristics of raw beef burger (St. Pierre and Kuhl, 2024). This optimal stiffness is critical for cultured meat production, as it provides the necessary structural support for cellular adhesion, proliferation, and differentiation, mimicking the physical cues required for muscle tissue development. Furthermore, the stress-relaxation properties of the scaffold, which have been demonstrated to influence cell behaviors such as migration, spreading, proliferation, and differentiation, have also been shown to maintain stability and durability under continuous mechanical load (Nam et al., 2019). This resilience is crucial for long-term cell cultivation, ensuring consistent support without structural degradation, which is advantageous for large-scale cultured meat production.

Biocompatibility represents a pivotal requirement for the fabrication of cell cultivation scaffolds. Despite the fact that all materials utilized in

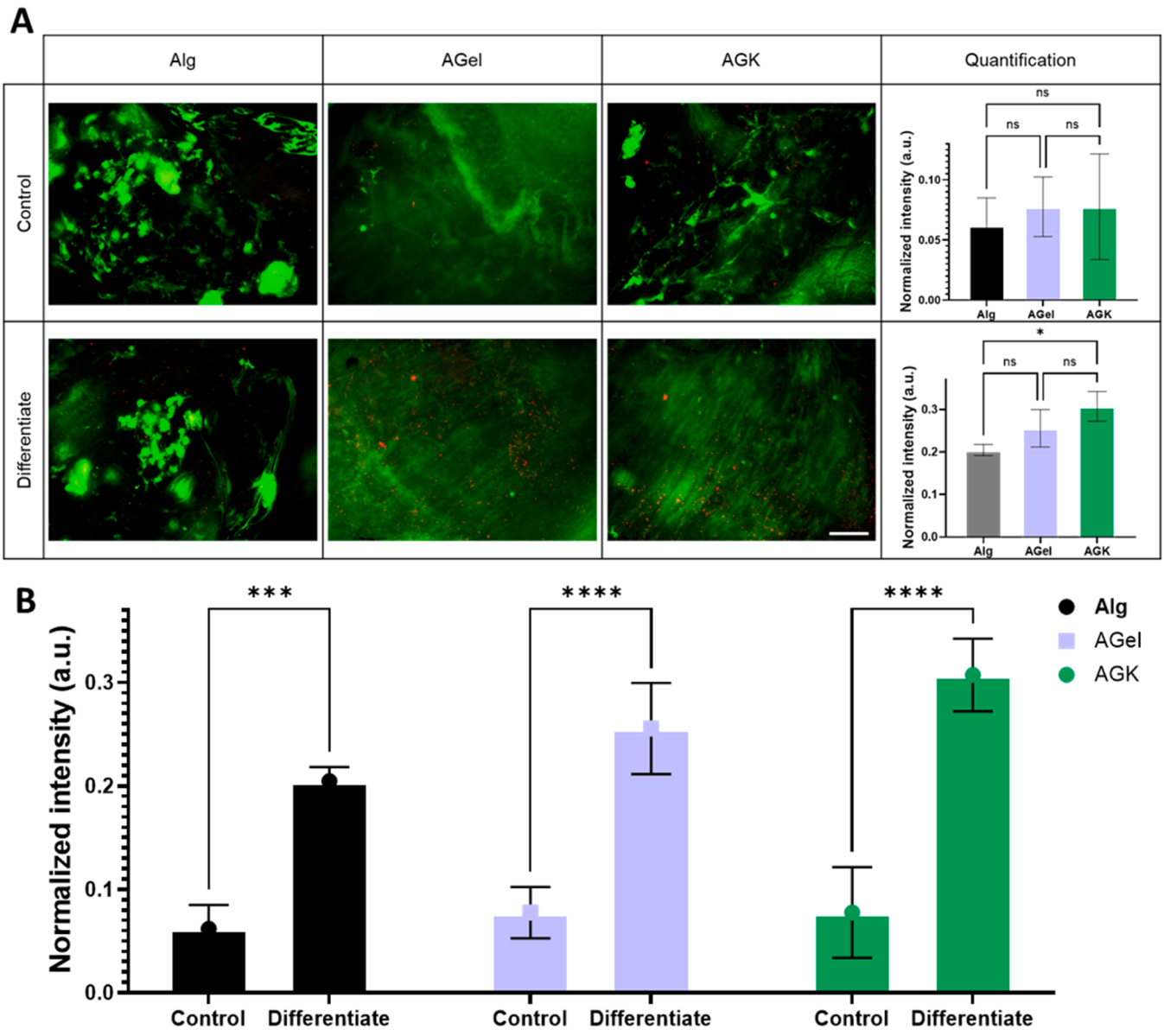

Fig. 7. C2C12 cell differentiation in scaffolds The differentiation potential of cells embedded in the scaffolds were analysed. MyoD1 as the early stage myogenesis biomarker was used to reveal the cell differentiation level. (A) Immunofluorescence staining was utilized to visualized the cell morphology and MyoD1 expression level (Green: F-Actin, Red: MyoD1, Scale bar: 500 μm) (B) The MyoD1 expression was quantified using ImageJ and normalized by actin signal. Statistical analysis was done with one-way (A) and two-way (B) ANOVA ($n = 3$, ns: no significant difference, *: $p < 0.05$, ***: $p < 0.005$, ****: $p < 0.001$).

the scaffold fabrication are FDA-approved as food-grade ingredients, additional testing is imperative due to the processing involved in scaffold preparation and its intended use for cell cultivation. In accordance with the report from Li et al. for indirect cytotoxicity testing, the pre-incubated medium from the scaffold was utilized to cultivate cells for a duration of 24 h (Li et al., 2022). The mitochondrial metabolic activity of the cells was then assessed through the implementation of a CCK-8 assay. Live/dead staining further confirmed cell viability, showing a high live cell ratio when cultured with the scaffold. These results collectively substantiate the safety and compatibility of the AGK scaffold for cellular applications. SEM images revealed that the AGK scaffold formed a complex network of thin fibers, offering more anchoring points for cell adhesion compared to the smoother surface of the alginate scaffold. This thin network construction has the capacity to simulate the structure of the extracellular matrix (ECM), thereby providing enhanced attachment property through mechanical support (Xie et al., 2022; Li et al., 2021).

For cultured meat production, a scaffold's ability to support muscle differentiation is critical. In this study, the observed upregulation of MyoD1 under differentiation conditions confirmed that the scaffold's microenvironment effectively promotes myogenic differentiation of C2C12 cells. Notably, MyoD1 expression levels in the AGK scaffold were significantly higher than those in the Alg scaffold, suggesting that AGK's fibrous, extracellular matrix–like architecture provides superior biochemical and mechanical cues for myogenesis (Jana et al., 2014). This aligns with previous findings demonstrating that scaffold architecture especially fiber density and alignment plays a pivotal role in influencing muscle cell behavior. The enhanced cellular alignment and increased signal intensity observed with AGK further reinforce its promise for cultured meat applications, particularly for engineering structured muscle tissue.

From a biological perspective, the AGK scaffold's superior mechanical and hydration properties significantly enhanced cell culture outcomes. Its elevated stiffness and thermal stability ensured efficient cell

attachment and proliferation, while the hydrated microenvironment supported cell viability and metabolic activity (Ko et al., 2021; Shi et al., 2017). The collective effect of these characteristics is to enhance the overall quality of cultured meat by creating a scaffold that combines mechanical resilience with biological compatibility. When compared to others polysaccharide-based scaffolds, AGK revealed outstanding cell viability and cell spreading (Lee et al., 2024; Grenier et al., 2023; Lin et al., 2023). The AGK scaffold integrates material robustness with biological performance, thereby addressing the dual challenges of cultured meat production: structural integrity and cellular support (Levi et al., 2022; Park et al., 2025). This study underscores the significance of selecting materials that not only exhibit mechanical durability but also facilitate an optimal environment for cell growth. The AGK scaffold exemplifies the transformative potential of plant-derived scaffolds in sustainable food production, combining sustainability, biocompatibility, and functionality.

In conclusion, the AGK scaffold signifies a substantial advancement in the domain of cultured meat production. By refining scaffold design and optimizing plant-based biomaterials, this study establishes the foundation for scalable and sustainable food systems, addressing the global demand for ethical and environmentally friendly protein sources. The findings emphasize the AGK scaffold's potential to propel progress in the realm of cultured meat technology, thereby paving the way for innovative, eco-friendly solutions in the food industry. Future improvements could focus on incorporating plant-proteins to further enhance the scaffold's bioactivity (Kong et al., 2024). The plant proteins, which are also highly sustainable and biocompatible, could provide additional support for cell adhesion (Han et al., 2024), and differentiation (Zheng et al., 2022), ultimately improving the texture and nutritional profile of cultured meat.

Ethical statement – studies in humans and animals

No animal and human studies were conducted to prepare this article.

CRediT authorship contribution statement

Kuo-Hui Chiu: Writing – review & editing, Writing – original draft, Visualization, Validation, Software, Methodology, Investigation, Formal analysis, Data curation, Conceptualization. **Szehon Anson Li:** Visualization, Validation, Methodology, Formal analysis, Data curation. **Stefan Schillberg:** Writing – review & editing, Supervision, Resources, Project administration, Funding acquisition, Conceptualization. **Che Julius Ngwa:** Writing – review & editing, Validation, Supervision, Resources, Project administration, Funding acquisition, Conceptualization.

Declaration of competing interest

The authors declare that they have no known competing financial interests or personal relationships that could have appeared to influence the work reported in this paper.

Acknowledgements

This work was supported by the European Union Horizon programme under the grant agreement no. 101136749 (FEASTS). The authors appreciate the technical support of mechanical testing from Prof. Dr. Horst Fischer from the Department of Dental Materials and Biomaterials Research, RWTH Aachen University Hospital, Aachen, Germany.

Supplementary materials

Supplementary material associated with this article can be found, in the online version, at doi:10.1016/j.fufo.2025.100795.

Data availability

Data will be made available on request.

References

Bhan, C., Asrey, R., Meena, N.K., Rudra, S.G., Chawla, G., Kumar, R., Kumar, R., 2022. Guar gum and chitosan-based composite edible coating extends the shelf life and preserves the bioactive compounds in stored Kinnow fruits. Int. J. Biol. Macromol. 222, 2922–2935.

Chen, C.-Y., Ke, C.-J., Yen, K.-C., Hsieh, H.-C., Sun, J.-S., Lin, F.-H., 2015. 3D porous calcium-alginate scaffolds cell culture system improved human osteoblast cell clusters for cell therapy. Theranostics 5, 643.

Chen, X., Li, L., Chen, L., Shao, W., Chen, Y., Fan, X., Liu, Y., Tang, C., Ding, S., Xu, X., 2023. Tea polyphenols coated sodium alginate-gelatin 3D edible scaffold for cultured meat. Food Res. Int. 173, 113267.

Chiu, K.-H., Karpat, M., Hahn, J., Chang, K.-Y., Weber, M., Wolf, M., Aveic, S., Fischer, H., 2023. Cyclic stretching triggers cell orientation and extracellular matrix remodeling in a periodontal ligament 3D In vitro model. Adv. Heal. Mater. 12, 2301422.

Fu, Y., Shen, Y., Chen, G., Wang, M., Li, X., Zhang, H., Ni, J., 2018. Effects of content of Na+ and Ca2+ on dynamic rheological properties of mixed gel system of konjac glucomannan and xanthan gum. Trans. Chin. Soc. Agric. Eng. 34, 301–307.

Gheorghita Puscaselu, R., Lobiuc, A., Dimian, M., Covasa, M., 2020. Alginate: from food industry to biomedical applications and management of metabolic disorders. Polymers 12, 2417.

Grenier, J., David, B., Journé, C., Cicha, I., Letourneur, D., Duval, H., 2023. Perfusion of MC3T3E1 preosteoblast spheroids within polysaccharide-based hydrogel scaffolds: an experimental and numerical study at the bioreactor scale. Bioengineering 10, 849.

Han, S.G., Lim, S.J., Hong, S.J., Kwon, H.C., Jung, H.S., Han, S.G., 2024. Comparison of soy and pea protein for cultured meat scaffolds: evaluating gelation, physical properties, and cell adhesion. Food Sci. Anim. Resour. 44, 1108.

Jahir, N.R., Ramakrishna, S., Abdullah, A.A.A., Vigneswari, S., 2023. Cultured meat in cellular agriculture: advantages, applications and challenges. Food Biosci. 53, 102614.

Jana, S., Leung, M., Chang, J., Zhang, M., 2014. Effect of nano-and micro-scale topological features on alignment of muscle cells and commitment of myogenic differentiation. Biofabrication 6, 35012.

Ke, C.-J., Chiu, K.-H., Chen, C.-Y., Huang, C.-H., Yao, C.-H., 2021. Alginate-gelatin based core-shell capsule enhances the osteogenic potential of human osteoblast-like MG-63 cells. Mater. Des. 210, 110109.

Kim, W.-J., Kim, Y., Ovissipour, R., Nitin, N., 2024. Plant-based biomaterials as scaffolds for cellular agriculture. Future Foods, 100468.

Kirsch, M., Morales-Dalmau, J., Lavrentieva, A., 2023. Cultivated meat manufacturing: technology, trends, and challenges. Eng. Life Sci. 23, e2300227.

Ko, H.J., Wen, Y., Choi, J.H., Park, B.R., Kim, H.W., Park, H.J., 2021. Meat analog production through artificial muscle fiber insertion using coaxial nozzle-assisted three-dimensional food printing. Food Hydrocoll. 120, 106898.

Kong, Y., Jing, L., Huang, D., 2024. Plant proteins as the functional building block of edible microcarriers for cell-based meat culture application. Crit. Rev. Food Sci. Nutr. 64, 4966–4976.

Lee, J.-Y., Kamel, J., Yadav, C.-J., Yadav, U., Afrin, S., Son, Y.-M., Won, S.-Y., Han, S.-S., Park, K.-M., 2024. Production of plant-based, film-type scaffolds using alginate and corn starch for the culture of bovine myoblasts. Foods 13, 1358.

Levi, S., Yen, F.-C., Baruch, L., Machluf, M., 2022. Scaffolding technologies for the engineering of cultured meat: towards a safe, sustainable, and scalable production. Trends. Food Sci. Technol. 126, 13–25.

Li, Z., Pearce, A.K., Dove, A.P., O'Reilly, R.K., 2021. Precise tuning of polymeric fiber dimensions to enhance the mechanical properties of alginate hydrogel matrices. Polymers 13, 2202.

Li, C.-H., Yang, I.-H., Ke, C.-J., Chi, C.-Y., Matahum, J., Kuan, C.-Y., Celikkin, N., Swieszkowski, W., Lin, F.-H., 2022. The production of fat-containing cultured meat by stacking aligned muscle layers and adipose layers formed from gelatin-soymilk scaffold. Front. Bioeng. Biotechnol. 10, 875069.

Lin, S.-P., Singajaya, S., Lo, T.-Y., Santoso, S.P., Hsu, H.-Y., Cheng, K.-C., 2023. Evaluation of porous bacterial cellulose produced from foam templating with different additives and its application in 3D cell culture. Int. J. Biol. Macromol. 234, 123680.

Madni, A., Khalid, A., Wahid, F., Ayub, H., Khan, R., Kousar, R., 2021. Preparation and applications of guar gum composites in biomedical, pharmaceutical, food, and cosmetics industries. Curr. Nanosci. 17, 365–379.

Mondal, K., Goswami, M., Goud, V.V., Katiyar, V., 2024. Optimization of guar gum-based anti-browning coating for prolonging the shelf life of cut potatoes. Int. J. Biol. Macromol. 269, 132051.

EFSA Panel on Food Additives and Nutrient Sources added to Food Mortensen, A., Aguilar, F., Crebelli, R., Di Domenico, A., Frutos, M.J., Galtier, P., Gott, D., Gundert-Remy, U., Lambré, C., 2017a. *Re*-evaluation of guar gum (E 412) as a food additive. EFSA J. 15, e04669.

EFSA Panel on Food Additives and Nutrient Sources added to Food Mortensen, A., Aguilar, F., Crebelli, R., Di Domenico, A., Frutos, M.J., Galtier, P., Gott, D., Gundert-Remy, U., Lambré, C., 2017b. *Re*-evaluation of konjac gum (E 425 i) and konjac glucomannan (E 425 ii) as food additives. EFSA J. 15, e04864.

Naahidi, S., Jafari, M., Logan, M., Wang, Y., Yuan, Y., Bae, H., Dixon, B., Chen, P., 2017. Biocompatibility of hydrogel-based scaffolds for tissue engineering applications. Biotechnol. Adv. 35, 530–544.
Nabil, M.E., Elsisy, S.F., Abd-Elrehim, M.A.-A., Abdelhady, N.H., 2025. Improvement of safety and quality of minced meat using pomegranate and guar gum extracts. Egypt. J. Vet. Sci. 1–13.
Nam, S., Stowers, R., Lou, J., Xia, Y., Chaudhuri, O., 2019. Varying PEG density to control stress relaxation in alginate-PEG hydrogels for 3D cell culture studies. Biomaterials 200, 15–24.
Ni, Y., Liu, Y., Zhang, W., Shi, S., Zhu, W., Wang, R., Zhang, L., Chen, L., Sun, J., Pang, J., 2021. Advanced konjac glucomannan-based films in food packaging: classification, preparation, formation mechanism and function. Lwt 152, 112338.
Park, S.M., Ryoo, J.H., Kwon, H.C., Han, S.G., 2025. Scaffold biomaterials in the development of cultured meat: a review. Food Sci. Anim. Resour.
Post, M.J., Levenberg, S., Kaplan, D.L., Genovese, N., Fu, J., Bryant, C.J., Negowetti, N., Verzijden, K., Moutsatsou, P., 2020. Scientific, sustainability and regulatory challenges of cultured meat. Nat. Food 1, 403–415.
Redondo, M., Presa, R., Granja, P.L., Araújo, M., Sousa, A., 2023. Konjac glucomannan photocrosslinked hydrogels for in vitro 3D cell culture. Mater. Today Chem. 34, 101761.
Savić Gajić, I.M., Savić, I.M., Svirčev, Z., 2023. Preparation and characterization of alginate hydrogels with high water-retaining capacity. Polymers 15, 2592.
Seah, J.S.H., Singh, S., Tan, L.P., Choudhury, D., 2022. Scaffolds for the manufacture of cultured meat. Crit. Rev. Biotechnol. 42, 311–323.
Senturk Parreidt, T., Müller, K., Schmid, M., 2018. Alginate-based edible films and coatings for food packaging applications. Foods. 7, 170.
Seo, J.W., Jung, W.K., Park, Y.H., Bae, H., 2023. Development of cultivable alginate fibers for an ideal cell-cultivated meat scaffold and production of hybrid cultured meat. Carbohydr. Polym. 321, 121287.
Shi, P., Laude, A., Yeong, W.Y., 2017. Investigation of cell viability and morphology in 3D bio-printed alginate constructs with tunable stiffness. J. Biomed. Mater. Res. A 105, 1009–1018.
St. Pierre, S.R., Kuhl, E., 2024. Mimicking mechanics: a comparison of meat and meat analogs. Foods 13, 3495.
Steinfeld, H., Wassenaar, T., 2007. The role of livestock production in carbon and nitrogen cycles. Annu. Rev. Env. Resour. 32, 271–294.
Tang, X., Deng, G., Yang, L., Wang, X., Xiang, W., Zou, Y., Lu, N., 2024. Konjac glucomannan-fibrin composite hydrogel as a model for ideal scaffolds for cell-culture meat. Food Res. Int. 187, 114425.
Thavamani, A., Sferra, T.J., Sankararaman, S., 2020. Meet the meat alternatives: the value of alternative protein sources. Curr. Nutr. Rep. 9, 346–355.
Wannasin, D., Ryu, J., McClements, D.J., 2024. Innovative method for producing plant-based meat analogs: acid/calcium-induced internal gelation of potato protein/alginate composites. Int. J. Biol. Macromol. 270, 132069.
Xie, Y., Kollampally, S.C.R., Jorgensen, M., Zhang, X., 2022. Alginate microfibers as therapeutic delivery scaffolds and tissue mimics. Exp. Biol. Med. 247, 2103–2118.
Zheng, Y.-Y., Shi, Y.-F., Zhu, H.-Z., Ding, S.-J., Zhou, G.-H., 2022. Quality evaluation of cultured meat with plant protein scaffold. Food Res. Int. 161, 111818.